Journal of Medicinal Chemistry

Article

pubs.acs.org/jmc

Huprine–Tacrine Heterodimers as Anti-Amyloidogenic Compounds of Potential Interest against Alzheimer's and Prion Diseases

Carles Galdeano,[†,‡] Elisabet Viayna,[†,‡] Irene Sola,[†,‡] Xavier Formosa,[†] Pelayo Camps,[†,‡] Albert Badia,[§] M. Victòria Clos,[§] Júlia Relat,[§] Míriam Ratia,[§] Manuela Bartolini,[∥] Francesca Mancini,[∥] Vincenza Andrisano,[∥] Mario Salmona,[⊥] Cristina Minguillón,[†] Gema C. González-Muñoz,[@] M. Isabel Rodríguez-Franco,[@] Axel Bidon-Chanal,[#] F. Javier Luque,[‡,#] and Diego Muñoz-Torrero*[,†,‡]

[†]Laboratori de Química Farmacèutica (Unitat Associada al CSIC), Facultat de Farmàcia, Universitat de Barcelona, Av. Diagonal 643, E-08028 Barcelona, Spain

[‡]Institut de Biomedicina (IBUB), Universitat de Barcelona, Barcelona, Spain

[§]Departament de Farmacologia, de Terapèutica i de Toxicologia, Institut de Neurociències, Universitat Autònoma de Barcelona, E-08193 Bellaterra, Barcelona, Spain

[∥]Department of Pharmaceutical Sciences, Alma Mater Studiorum, Bologna University, Via Belmeloro 6, I-40126 Bologna, Italy

[⊥]Department of Molecular Biochemistry and Pharmacology, Istituto di Ricerche Farmacologiche "Mario Negri", Milan, Italy

[@]Instituto de Química Médica (IQM-CSIC), Juan de la Cierva, 3, E-28006 Madrid, Spain

[#]Departament de Fisicoquímica, Facultat de Farmàcia, Universitat de Barcelona, Av. Diagonal 643, E-08028 Barcelona, Spain

Supporting Information

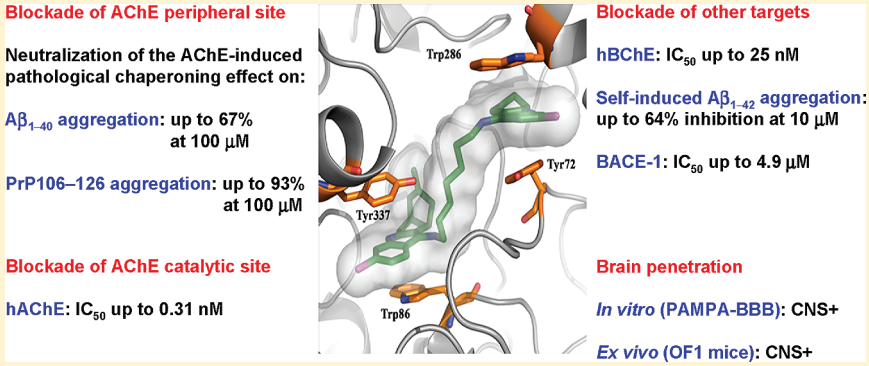

ABSTRACT: A family of huprine–tacrine heterodimers has been developed to simultaneously block the active and peripheral sites of acetylcholinesterase (AChE). Their dual site binding for AChE, supported by kinetic and molecular modeling studies, results in a highly potent inhibition of the catalytic activity of human AChE and, more importantly, in the in vitro neutralization of the pathological chaperoning effect of AChE toward the aggregation of both the β-amyloid peptide (Aβ) and a prion peptide with a key role in the aggregation of the prion protein. Huprine–tacrine heterodimers take on added value in that they display a potent in vitro inhibitory activity toward human butyrylcholinesterase, self-induced Aβ aggregation, and β-secretase. Finally, they are able to cross the blood–brain barrier, as predicted in an artificial membrane model assay and demonstrated in ex vivo experiments with OF1 mice, reaching their multiple biological targets in the central nervous system. Overall, these compounds are promising lead compounds for the treatment of Alzheimer's and prion diseases.

INTRODUCTION

Alzheimer's disease (AD) and prion diseases are fatal progressive neurodegenerative disorders with a devastating albeit very different impact on humans. Worldwide, it is estimated that 35 million people suffer dementia, most cases being due to AD,[1] whereas prion diseases affect approximately one individual in 1 million people each year.[2] Although relatively rare, the emergence of variant Creutzfeldt-Jakob disease in the human population likely due to the consumption of contaminated beef products has attracted much scientific and public interest. The devastating nature and public health concerns posed by Alzheimer's and prion diseases render the development of effective drugs against these disorders an acute clinical need.[3]

Very interestingly, despite the significant differences in incidence, as well as in clinical symptomatology and disease evolution, AD and prion diseases share common hallmarks and

Received: June 28, 2011
Published: December 19, 2011

similar pathogenic mechanisms,[4,5] among them oxidative stress, excessive transition metal ions, and prominently aggregation and accumulation in the brain of a β-sheet rich protein as fibrillar amyloid deposits, namely the β-amyloid peptide (Aβ) in AD, a 39−43-amino acid peptide arising from the proteolytic cleavage of the amyloid precursor protein (APP) by the sequential action of the enzymes β-secretase (BACE-1) and γ-secretase, and the scrapie prion protein (PrP^{Sc}), a conformationally altered isoform of the 209-amino acid normal cellular prion protein (PrP^{C}).[2,5,6] Consequently, similar therapeutic approaches against Alzheimer's and prion diseases could be envisaged, including antioxidants, β-sheet breakers, and metal chelators.[4,6,7]

Because aggregation of misfolded Aβ or PrP^{Sc} is widely accepted to be a key event in the early pathogenesis of Alzheimer's and prion diseases,[2,8] anti-AD and anti-prion drug discovery is to a large extent driven by the design of Aβ and prion protein aggregation inhibitors. Thus, Aβ aggregation inhibitors have been extensively studied in the past,[9] whereas the design of prion protein anti-aggregating compounds is becoming increasingly popular,[10] by disruption of protein−protein interactions through a direct action on the protein prone to aggregation. However, the conversion of soluble Aβ or PrP^{C} into each pathological β-sheet rich conformer and their subsequent aggregation can be promoted by the action of pathological chaperones.[3] Indeed, apolipoprotein E (apoE),[11] α1-antichymotrypsin,[11] C1q complement factor,[12] and acetylcholinesterase (AChE)[13] have been reported to accelerate Aβ aggregation in vitro. Very interestingly, a critical dependence of Aβ deposition in plaques on the presence of apoE and AChE has also been confirmed in vivo in transgenic mice models of AD.[14,15] The pathological chaperoning effect of apoE and AChE seems to be initiated by the binding to Aβ through hydrophobic interactions to form stable complexes that are prone to aggregation.[13,16,17] Inhibition of the pathological chaperoning effect of these molecules by blockade of these hydrophobic interactions has emerged as a promising approach to reducing the level of protein aggregation and modifying disease progression at a very early stage.[8] Binding of AChE to Aβ is proposed to be mediated by the AChE peripheral site,[16] located at the mouth of a 20 Å narrow gorge at the bottom of which the catalytic site is placed. Thus, compounds able to block either the AChE peripheral site or simultaneously both the catalytic and peripheral sites [dual-binding site AChE inhibitors (AChEIs)] have emerged as promising new drug candidates for mitigating the pathological chaperoning effect of AChE. The proof of concept of this approach has been obtained from a few dual-binding site AChEIs,[18−20] which have been shown to reduce brain amyloid load and improve cognition in animal models of AD. One of them, Noscira's NP-61, is currently in phase I clinical trials for AD in the United Kingdom.

It remains to be determined whether a similar approach can be used against prion diseases. A first step in this direction has been the recent discovery of a similar pathological chaperoning effect of AChE toward prion peptide aggregation. Thus, AChE has been reported to promote in vitro the aggregation of PrP106−126,[21] one of the key domains involved in the aggregation and conformational change of the prion protein, and PrP82−146, the main component of the amyloid plaques found in patients with Gerstmann-Sträussler-Scheinker disease, accelerating oligomer and amyloid fibril formation.[22] Not unlike the interaction with Aβ, the PrP pro-aggregating action of AChE seems to reside in its peripheral site, as addition of the specific peripheral site inhibitor propidium iodide results in the inhibition of AChE-induced PrP106−126 and PrP82−146 aggregation. Thus, at 100 μM, propidium iodide inhibits the AChE-induced aggregation of Aβ,[23] PrP106−126,[21] and PrP82−146[22] by 82, 87, and 78%, respectively. However, because of its DNA−RNA intercalating properties and the presence of two quaternary nitrogen atoms, which prevents its entry into the central nervous system (CNS), propidium iodide does not have any therapeutic applicability. Alternatively, dual-binding site AChEIs should also be able to inhibit the AChE-induced PrP aggregation, although no example of such a class of compounds with this activity has been reported.

Recently, we described a short series of dual-binding site AChEIs,[24] consisting of a unit of racemic huprine Y [(±)-**6** (Scheme 1)], a high-affinity reversible AChEI,[25] and a unit of tacrine [**1** (Scheme 1)], a known AChEI with reported affinity for both the active and peripheral sites of AChE,[26] or its 6-chloro-substituted analogue, 6-chlorotacrine (**2**), connected through a linker of suitable length. These racemic huprine−tacrine heterodimers exhibited a very potent inhibitory activity toward human erythrocyte AChE and human serum butyrylcholinesterase (BChE),[24] although their mechanism of action, i.e., the dual-site binding to AChE, as well as their anti-amyloidogenic effects remained to be determined.

Scheme 1. Synthesis of the Huprine−Tacrine Heterodimers

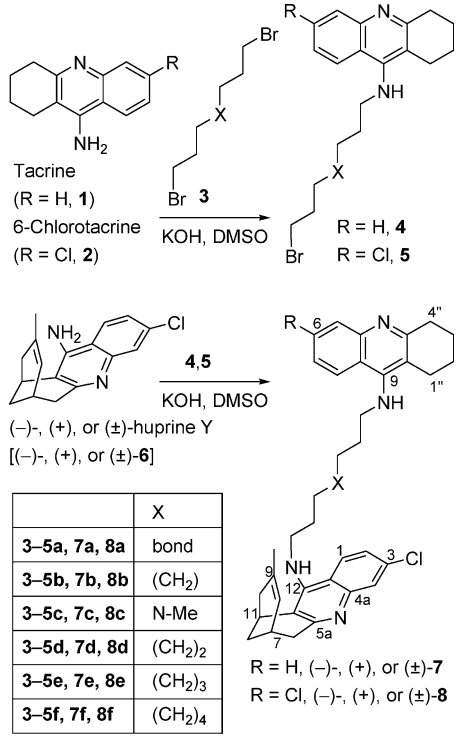

	X
3–5a, 7a, 8a	bond
3–5b, 7b, 8b	(CH_2)
3–5c, 7c, 8c	N-Me
3–5d, 7d, 8d	$(CH_2)_2$
3–5e, 7e, 8e	$(CH_2)_3$
3–5f, 7f, 8f	$(CH_2)_4$

Herein, we describe the synthesis of several enantiopure huprine−tacrine heterodimers and new longer racemic homologues, as well as a thorough pharmacological evaluation of the new heterodimers and those previously reported, including, on one hand, the determination of their inhibitory activity toward AChE-induced Aβ and PrP aggregation and toward human recombinant AChE. The mechanism of action responsible for these activities has been studied by means of molecular dynamics simulations and kinetic studies. On the

dx.doi.org/10.1021/jm200840c | J. Med. Chem. 2012, 55, 661−669

Table 1. Inhibitory Activities of the Dihydrochlorides or Trihydrochlorides of Huprine−Tacrine Heterodimers and Reference Compounds toward AChE and AChE-Induced $A\beta_{1-40}$ and PrP106−126 Aggregation, BChE, Self-Induced $A\beta_{1-42}$ Aggregation, and BACE-1[a]

compd	hAChE IC_{50} (nM)[b]	AChE-induced $A\beta_{1-40}$ aggregation[c] (%)	AChE-induced PrP106−126 aggregation[c] (%)	hBChE IC_{50} (nM)[b]	$A\beta_{1-42}$ self-induced aggregation[d] (%)	BACE-1 inhibition[e] (%)
(±)-**7a**	0.89 ± 0.07	44.4 ± 1.3	90.9 ± 2.0	24.6 ± 1.5	44.4 ± 7.0	na[f]
(±)-**7b**	1.89 ± 0.19	56.9 ± 5.1	89.1 ± 2.5	87.1 ± 4.2	51.5 ± 3.1	na[f]
(−)-**7b**	1.33 ± 0.07	66.4 ± 1.3	91.1 ± 1.3	133 ± 4.1	60.8 ± 6.4	na[f]
(+)-**7b**	6.84 ± 0.48	56.5 ± 3.0	83.5 ± 3.4	139 ± 5.2	57.0 ± 7.2	na[f]
(±)-**7c**	0.42 ± 0.04	38.8 ± 3.7	92.4 ± 0.6	44.2 ± 1.3	28.1 ± 6.4	na[f]
(±)-**7d**	1.38 ± 0.13	66.9 ± 1.3[g]	87.3 ± 2.8[h]	74.2 ± 5.7	63.7 ± 4.0	na[f]
(±)-**7e**	3.53 ± 0.37	57.8 ± 0.4	87.2 ± 2.9	43.3 ± 4.2	53.7 ± 0.9	26.5 ± 1.6
(±)-**7f**	4.19 ± 0.39	54.1 ± 0.3	93.4 ± 1.2	26.6 ± 2.5	33.3 ± 4.9	34.8 ± 2.5[i]
(±)-**8a**	0.74 ± 0.07	30.0 ± 3.7	91.9 ± 1.4	75.2 ± 2.6	30.9 ± 2.2	18.5 ± 3.5
(±)-**8b**	4.02 ± 0.27	44.2 ± 5.7	84.5 ± 3.9	73.3 ± 6.0	37.0 ± 5.7	40.9 ± 0.4
(−)-**8b**	2.04 ± 0.24	42.7 ± 1.1	79.4 ± 8.3	86.8 ± 4.2	32.2 ± 2.7	40.0 ± 2.8[j]
(+)-**8b**	11.5 ± 1.08	44.9 ± 2.2	83.1 ± 5.5	47.4 ± 4.4	45.5 ± 3.6	41.8 ± 0.7[k]
(±)-**8c**	0.31 ± 0.02	35.2 ± 2.9	87.5 ± 2.2	51.3 ± 4.6	38.6 ± 5.5	na[f]
(±)-**8d**	1.32 ± 0.09	47.2 ± 1.4	87.2 ± 2.6[l]	35.1 ± 3.8	30.3 ± 0.2	46.6 ± 3.1[m]
(±)-**8e**	3.26 ± 0.19	23.5 ± 0.4	91.7 ± 2.5	27.2 ± 2.3	36.3 ± 4.0	41.6 ± 1.0[n]
(±)-**8f**	9.09 ± 0.92	23.4 ± 2.3	90.4 ± 1.3	76.6 ± 4.9	29.3 ± 4.7	40.3 ± 0.1[o]
(±)-**6**	0.69 ± 0.03	17.1 ± 4.5	69.0 ± 1.3	175 ± 6.3	nd[p]	nd[p]
(−)-**6**	0.43 ± 0.03	24.7 ± 1.3	nd[p]	nd[p]	11.5 ± 5.2	14.0 ± 0.1
(+)-**6**	13.6 ± 1.50	9.1 ± 3.6	nd[p]	nd[p]	13.2 ± 1.9	13.6 ± 2.3
1	317 ± 15.3	5.2 ± 2.9	16.2 ± 1.7	24.5 ± 0.6	5.6 ± 1.6	na[f]

[a]Values are expressed as means ± the standard error of the mean (SEM) of at least four experiments (n = 4), each performed in duplicate (AChE and BChE inhibition), three experiments (n = 3), each performed in duplicate (AChE-induced, self-induced $A\beta$ aggregation, and BACE-1 inhibition), or three experiments (n = 3), each performed in triplicate (AChE-induced PrP106−126 aggregation inhibition). [b]IC_{50} inhibitory concentration of human recombinant AChE or human serum BChE. [c]Percent inhibition with inhibitor at 100 μM. [d]Percent inhibition with inhibitor at 10 μM (5:1 [$A\beta$]:[I]). [e]Percent inhibition with inhibitor at 5 μM, and human recombinant BACE-1 (Sigma) and substrate M-2420 (Bachem) (for huprine−tacrine heterodimers) or human recombinant BACE-1 (Invitrogen) and substrate Panvera Peptide (Invitrogen) (for reference compounds). [f]Not active. [g]IC_{50} = 61.3 ± 5.4 μM. [h]IC_{50} = 68.7 ± 1.0 nM. [i]IC_{50} = 7.3 ± 0.8 μM. [j]IC_{50} = 5.7 ± 0.5 μM. [k]IC_{50} = 5.9 ± 1.1 μM. [l]IC_{50} = 263 ± 50 nM. [m]IC_{50} = 4.9 ± 0.6 μM. [n]IC_{50} = 5.8 ± 1.2 μM. [o]IC_{50} = 6.6 ± 0.1 μM. [p]Not determined.

other hand, other anti-amyloidogenic activities such as the inhibitory activities toward $A\beta$ self-induced aggregation and BACE-1 as well as the BChE inhibitory activity have been evaluated for the whole family of huprine−tacrine heterodimers. Finally, the penetration of these compounds into the brain has been assessed using an artificial membrane assay and ex vivo experiments.

RESULTS AND DISCUSSION

Chemistry. The previously described huprine−tacrine heterodimers bear a unit of racemic huprine Y and a hexa-, hepta-, 4-methyl-4-azahepta-,[27] or octamethylene linker [(±)-**7a−d** and (±)-**8a−d** (Scheme 1)]. With regard to the interaction with the catalytic site of AChE, it is well established that the eutomer in the family of huprines is the levorotatory enantiomer, bearing the 7*S*,11*S* configuration.[25,28,29]

In this work, we have synthesized the new longer nona- and decamethylene-linked homologues in racemic form [(±)-**7e**, (±)-**7f**, (±)-**8e**, and (±)-**8f**], as well as the enantiopure (−)-(7*S*,11*S*)- and (+)-(7*R*,11*R*)-heptamethylene-linked heterodimers (−)-**7b**, (+)-**7b**, (−)-**8b**, and (+)-**8b** (Scheme 1), to determine if longer tether lengths could lead to improved blockade of the AChE peripheral site upon dual-site binding to the enzyme and to assess potential differences in potency between the enantiomers of huprine−tacrine heterodimers with respect to the different biological activities to be tested.

As previously described,[24] the synthesis of the new huprine−tacrine heterodimers was envisaged by nucleophilic substitution of α,ω-dihaloalkanes with 4-aminoquinoline derivatives tacrine or 6-chlorotacrine and huprine Y. Alternative procedures based on the high-temperature nucleophilic aromatic substitution of 4-chloroquinoline derivatives with α,ω-diaminoalkanes[30] or Pd-catalyzed amination reactions[31,32] were discarded because they required the use of a huprine-related 4-chloroquinoline precursor not readily available.[24]

Thus, alkylation of tacrine (**1**) or 6-chlorotacrine (**2**)[33] with 1,9-dibromononane or 1,10-dibromodecane in the presence of KOH in DMSO[26] afforded bromoalkyltacrines **4e,f** and **5e,f** in moderate yields (Scheme 1). Alkylation of racemic huprine Y,[34] (±)-**6**, with **4e,f** and **5e,f** under similar reaction conditions, followed by purification via silica gel column chromatography, afforded the racemic heterodimers (±)-**7e,f** and (±)-**8e,f** in moderate to good yields.

Different attempts to chromatographically resolve (±)-**8b** at preparative scale by medium-pressure liquid chromatography (MPLC) using microcrystalline cellulose triacetate as the chiral stationary phase[34] under different conditions were fruitless. Eventually, we managed to set up a novel methodology that allowed the resolution of (±)-**8b**, based on preparative high-performance liquid chromatography (HPLC) using amylose tris(3,5-dimethylphenylcarbamate) as the chiral selector in the stationary phase and a 100:0.2 acetonitrile/Et_2NH mixture as the eluent, which afforded (−)-**8b** and (+)-**8b** in >99 and 97% ee, respectively, albeit in insufficient amounts to allow their complete chemical and pharmacological characterization. Alternatively, enantiopure heterodimers (−)- and (+)-**7b** and (−)- and (+)-**8b** were prepared at a more suitable scale (decigram scale) and in good yields by chromatographic

dx.doi.org/10.1021/jm200840c | J. Med. Chem. 2012, 55, 661−669

resolution of huprine Y, (±)-**6**, by our previously described methodology,[34] followed by alkylation of the obtained enantiopure (−)- or (+)-**6** with bromoheptyltacrine **4b** or **5b**, respectively (Scheme 1).

The novel huprine−tacrine heterodimers were fully characterized as dihydrochlorides via their spectroscopic data and elemental analyses. Pharmacological evaluation of the complete family of huprine−tacrine heterodimers was conducted from their dihydrochloride or trihydrochloride salts.

Pharmacology and Molecular Modeling. *Inhibition of Human AChE and AChE-Induced Aβ and PrP Aggregation. AChE Inhibition.* Huprine−tacrine heterodimers were rationally designed to hit AChE as their primary biological target, in a dual-site binding fashion, which should endow these compounds with the ability to block the enzyme catalytic activity and, more interestingly, the pathological chaperoning effect of AChE toward both Aβ and PrP aggregation. The AChE inhibitory activity of the novel heterodimers (±)-**7e,f**, (±)-**8e,f**, (−)-**7b**, (+)-**7b**, (−)-**8b**, and (+)-**8b** was assayed by the method of Ellman et al.[35] on human recombinant AChE (hAChE) (Table 1). Also, the previously synthesized heterodimers (±)-**7a−d** and (±)-**8a−d**, which had been evaluated using human erythrocyte AChE, were re-evaluated using the more readily available human recombinant enzyme.

All the huprine−tacrine heterodimers are very potent inhibitors of human recombinant AChE, exhibiting IC_{50} values in the subnanomolar to low nanomolar range. The presence or absence of a chlorine atom at position 6 of the tacrine unit does not seem to have a clear effect on hAChE inhibitory activity, thus suggesting that the tacrine unit is binding at the AChE peripheral site, rather than the active site. Conversely, some clear trends were found regarding the length and nature of the linker of these heterodimers. On one hand, the inhibitory activity was maximal when a chain of six methylenes was present and decreased in the longer homologues, heterodimers (±)-**7a** and (±)-**8a** being 5- and 12-fold more potent than decamethylene-linked heterodimers (±)-**7f** and (±)-**8f**, respectively. A second peak of activity was found for octamethylene-linked heterodimers (±)-**7d** and (±)-**8d**, which turned out to be 3- and 7-fold more potent than (±)-**7f** and (±)-**8f**, respectively. On the other hand, replacement of the central methylene group of the tether chain of heptamethylene-linked compounds (±)-**7b** and (±)-**8b** with a protonatable methylamino group, (±)-**7c** and (±)-**8c**, respectively, resulted in 5- and 13-fold increased hAChE inhibitory potency, respectively. These results are in agreement with those reported by Savini et al. for a series of tacrine homodimers and may be ascribed to additional cation−π interactions with some midgorge aromatic residues, which would act as a third recognition site within the active site gorge of AChE, apart from the active and peripheral sites.[27] As expected, the levorotatory (7*S*,11*S*)-huprine-based heterodimers are the eutomers with regard to hAChE inhibition, compounds (−)-**7b** and (−)-**8b** being 5−6-fold more potent than the dextrorotatory enantiomers.

Overall, the most potent huprine−tacrine heterodimers are (±)-**7c** and (±)-**8c**, which turned out to be ∼2- and ∼750−1000-fold more potent than the parent (±)-huprine Y and tacrine, respectively, and (±)-**7a** and (±)-**8a**, which were roughly equipotent to (±)-huprine Y and around 400-fold more potent than tacrine.

AChE-Induced Aβ Aggregation Inhibition. The ability of the huprine−tacrine heterodimers to block the chaperoning effect of AChE toward $A\beta_{1-40}$ aggregation was assessed using a thioflavin T fluorescent method,[23] and the parent racemic and enantiopure huprines and tacrine as reference compounds (Table 1). Huprine−tacrine heterodimers, at 100 μM, exhibited a significant inhibitory activity toward hAChE-induced Aβ aggregation, with percentages of inhibition ranging from 39 to 67% in the tacrine-based heterodimers and from 23 to 47% in the chlorotacrine-based heterodimers. All heterodimers are clearly more potent Aβ anti-aggregating compounds than the parent huprine Y and tacrine. The structural features leading to a stronger Aβ anti-aggregating effect are the presence of an unsubstituted tacrine unit and an octamethylene linker, heterodimer (±)-**7d** being the most potent of the family (IC_{50} = 61.3 ± 5.4 μM.). In contrast with the trends found regarding hAChE inhibition, (i) the presence of a protonatable amino group within the linker seems to be detrimental for the AChE-induced Aβ aggregation inhibitory activity and (ii) there are no significant differences in Aβ anti-aggregating activity between enantiomeric huprine−tacrine heterodimers.

AChE-Induced PrP106−126 Aggregation Inhibition. The ability of the huprine−tacrine heterodimers to block the chaperoning effect of AChE toward PrP106−126 aggregation was assessed through fluorescence microscopy analysis using a peptide containing a coumarin fluorescent probe (coumarin PrP106−126) and bovine AChE.[21] The parent racemic and enantiopure huprines as well as tacrine were also evaluated as reference compounds (Table 1). All the huprine−tacrine heterodimers, at 100 μM, turned out to be potent inhibitors of the AChE-induced PrP106−126 aggregation with percentages of inhibition generally higher than 80%, and, therefore, without significant differences between compounds bearing an unsubstituted or chloro-substituted tacrine unit, between different tether lengths, or between enantiomers. To the best of our knowledge, this is the first report of a family of dual-binding site AChEIs able to neutralize the pathological chaperoning effect of AChE toward both Aβ and PrP aggregation.

Even though huprine−tacrine heterodimers are more potent Aβ and PrP anti-aggregating compounds than the parent tacrine and huprine Y, the latter compound exhibits a remarkable inhibitory activity (17 and 69% inhibition of AChE-induced Aβ and PrP106−126 aggregation, respectively). Indeed, huprine X, the 9-ethyl-substituted analogue of huprine Y, has recently been reported to decrease by 40% levels of insoluble $A\beta_{1-40}$ in the hippocampus of a transgenic mouse model of AD.[36] (−)-Huprine X has been shown to tightly bind to the AChE active site,[29] but kinetic studies have demonstrated that this compound also interferes with the binding of the peripheral site AChEI propidium to AChE.[25] The binding geometry and added molecular volume of huprines, when bound to the active site, could therefore account for the decreased affinity of peripheral site ligands such as propidium, which could also be the case for Aβ and PrP.

The potent and greater (relative to the parent huprine Y and tacrine) inhibitory activity of huprine−tacrine heterodimers toward hAChE and AChE-induced Aβ and PrP aggregation might be ascribed to dual-site binding to the enzyme.

Kinetic Analysis of AChE Inhibition. To gain insight into the mechanism of action of the huprine−tacrine heterodimers, responsible for AChE inhibition as well as AChE-induced Aβ and PrP aggregation, we conducted both kinetic analysis and molecular modeling studies of the interaction of selected compounds with hAChE. The mechanism of AChE inhibition

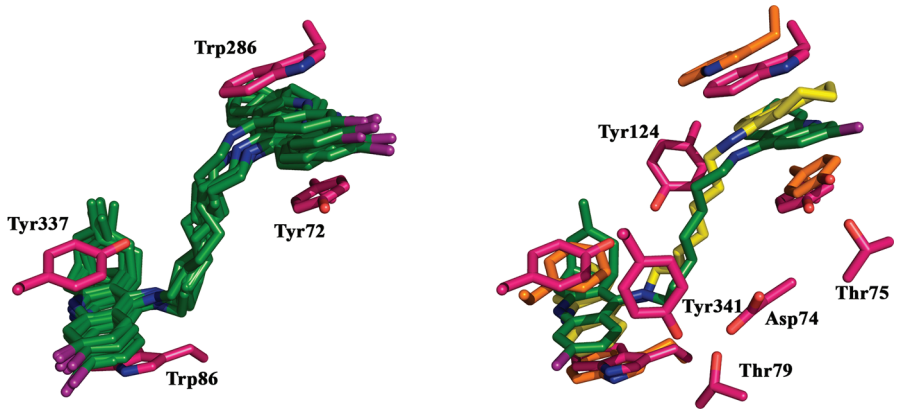

Figure 1. Representation of the mode of binding of (−)-**8b** (green) in the catalytic gorge of hAChE. The left panel shows the superposition of the snapshots at the beggining and end of the 34 ns trajectory, and of the snapshots taken every 5 ns. The right panel shows the superposition of bis(7)-tacrine (yellow) and (−)-**8b** in the final snapshot of the trajectory (magenta) and X-ray structure 2CKM (orange). The side chains of selected residues are also shown (hydrogens omitted for the sake of clarity).

was investigated in vitro using compound (−)-**8b**. Graphical analysis of the overlaid reciprocal Lineweaver−Burk plots (Figure S2 of the Supporting Information) showed both increasing slopes (decreased V_{max}) and increasing intercepts (higher K_m) at increasing inhibitor concentrations, this pattern being indicative of a mixed-type inhibition. Thus, this kinetic study supported the dual-site binding to AChE as the mechanism of action of this compound. Replots of the slope versus concentration of (−)-**8b** give an estimate of the competitive inhibition constant, K_i, of 1.51 nM.

Molecular Modeling Studies. The mechanism of action of huprine−tacrine heterodimer (−)-**8b** on AChE was further studied by molecular dynamics (MD) simulations. To this end, the orientation of the inhibitor in the catalytic gorge of AChE was modeled by taking advantage of the X-ray structural data available for distinct AChE−ligand complexes. The X-ray structure of the complex between *Torpedo californica* AChE (*Tc*AChE) and the heptamethylene-linked bis(4-aminoquinoline)-based compound bis(7)-tacrine (PDB entry 2CKM)[37] was used as template to orient (−)-**8b**. Both huprine and 6-chlorotacrine units in (−)-**8b** should be capable of interacting simultaneously at both catalytic and peripheral sites of the enzyme, thus mimicking the interaction of the two tacrine units of bis(7)-tacrine with Trp84 (catalytic site; Trp86 in hAChE) and Trp279 (peripheral site; Trp286 in hAChE). Taking into account the larger hAChE inhibitory activity of (−)-huprine Y relative to that of 6-chlorotacrine (31-fold more potent against recombinant hAChE, as the experimentally measured IC_{50} of 6-chlorotacrine is 13.2 nM), we placed the huprine Y moiety of (−)-**8b** in the catalytic site and its 6-chlorotacrine unit in the peripheral site. From a structural viewpoint, the 4-aminoquinoline unit of (−)-huprine X bound to *Tc*AChE (PDB entry 1E66)[29] superposes well with the corresponding unit of tacrine in its complex with *Tc*AChE (PDB entry 1ACJ),[38] and with the tacrine moiety of bis(7)-tacrine that fills the active site in 2CKM. This arrangement permits the carbobicyclic system of (−)-huprine X to be accommodated in a pocket defined by aromatic residues Phe288, Phe290, and Phe331, whereas the chlorine atom at position 3 fills a hydrophobic pocket delineated by Trp432 and Met436 (Figure S3 of the Supporting Information). A similar arrangement might be expected for the binding of the huprine moiety of (−)-**8b** to the catalytic site. With regard to the peripheral site interacting unit, two orientations that differ by a 180° rotation around the N−N axis of the central ring of the 6-chlorotacrine unit of (−)-**8b** were considered (Figure S3 of the Supporting Information), namely, a first binding mode in which the chlorine atom was oriented toward the aqueous solvent (denoted as binding mode **A**) and an alternative binding mode in which the chlorine atom was oriented toward the interior of the peripheral site (denoted as binding mode **B**). In both orientations, the 6-chlorotacrine moiety would stack against Trp279 and Tyr70 (Trp286 and Tyr72, respectively, in hAChE). However, the pseudoplanar structure of the 6-chlorotacrine moiety and the large accessibility of the peripheral site make it difficult to discern a priori between the two arrangements in the peripheral site.

After 34 ns MD simulations of these two alternative modes of binding of (−)-**8b** to hAChE, orientation **A** seemed to be the most favorable. The reliability of this binding mode is supported by the structural integrity and energetic stability of the snapshots collected from the trajectory (Figure 1 and Figure S4 of the Supporting Information). The root-mean-square deviation (rmsd) of the protein backbone amounts to 1.9 Å, which is slightly larger than the rmsd determined for the set of residues that delineate the binding cavity, including catalytic, midgorge, and peripheral sites (1.4 Å). The heteroaromatic ring system of the (−)-huprine moiety is firmly stacked against the indole ring of Trp86 (average distance of 4.0 Å) and the phenol ring of Tyr337 (average distance of 3.8 Å). Moreover, the stacked complex is further stabilized by the hydrogen bond between the protonated quinoline nitrogen atom and the carbonyl group of His447 (2.9 Å). On the other hand, the 6-chlorotacrine unit remains stacked against the aromatic rings of Trp286 and Tyr72 (average distances of 3.7 and 3.8 Å, respectively). Even though there are no specific interactions between the heptamethylene linker and the residues in the midgorge, it is worth noting that the structural integrity of the binding site is assisted by a network of transient hydrogen bonds between different residues, namely, hydrogen bonds between Asp74 and Tyr341 and Thr79, a hydrogen bond between Tyr72 and Thr75, and finally a water-mediated bridge between Tyr337 and Tyr124. Compared to the X-ray structure of the *Tc*AChE−bis(7)-tacrine complex, it is worth noting the global resemblance found between the skeleton of (−)-**8b** in the modeled complex and bis(7)-tacrine in the X-ray structure (Figure 1), as noted in the similar position of the heteroaromatic rings and the heptamethylene linker. Overall,

dx.doi.org/10.1021/jm200840c | *J. Med. Chem.* 2012, 55, 661−669

the structural analysis supports the stability of binding mode **A** proposed for (−)-**8b** in hAChE.

When the alternative binding mode **B** was examined, the rmsd profile revealed the occurrence of much larger structural readjustment in the residues that delineate the binding site (Figure S5 of the Supporting Information), which is clearly visible in the distorted structure of the ligand and relevant residues in the binding site (Figure S6 of the Supporting Information). This effect can be ascribed to the unfavorable interactions between the chlorine atom of the 6-chlorotacrine unit and the carboxylate and carbonyl groups of Glu285 and Val282, respectively, which tend to displace the tacrine unit from the peripheral site. Such displacement alters the arrangement of the side chain, which in turn leads to steric clashes in the midgorge and is propagated to the catalytic site (Figure S7 of the Supporting Information).

From an energetic point of view, the larger structural stability of binding mode **A** is also reflected in the binding affinities predicted using the solvent interaction energy (SIE) technique, which is a variant of the MM/PBSA method carefully parametrized by calibrating the (free) energy contributions against experimental binding affinities.[39] The SIE calculations were performed for 100 snapshots evenly taken during the last 5 ns of the trajectories. Whereas the binding affinity ($\Delta G_{binding}$) is predicted to be −14.4 ± 0.3 kcal/mol for binding mode **A**, it is destabilized by 1.6 kcal/mol ($\Delta G_{binding}$ = −12.8 ± 0.5 kcal/mol) for binding mode **B**, thus reinforcing the integrity of binding mode **A** for the AChE−(−)-**8b** complex.

BChE Inhibition. Other activities of interest in the context of AD treatment such as BChE, self-induced Aβ aggregation, and BACE-1 inhibition have been also evaluated (Table 1).

There is a growing appreciation of an important role of BChE in dementia, where this enzyme seems to exert a compensatory effect in response to a great decrease in brain AChE activity as AD progresses.[40] In this light, the inhibitory activity of the huprine−tacrine heterodimers on human serum BChE (hBChE) was assayed by the method of Ellman et al. (Table 1).[35]

(±)-Huprine Y inhibits hAChE 250-fold more potently than hBChE. The presence of the chlorine atom at position 3 of the aminoquinoline moiety of huprines, which is in part responsible for its high hAChE inhibitory activity,[29] becomes detrimental for hBChE inhibition. A steric hindrance between the chlorine atom and the side chain of Met437 in the hBChE active site seems to account for the detrimental effect of this substituent on the hBChE inhibitory activity of chloro-substituted 4-aminoquinolines relative to unsubstituted counterparts such as tacrine,[27,41] which turned out to be 13-fold more potent toward hBChE than hAChE. As huprines, huprine−tacrine heterodimers are selective inhibitors of hAChE, exhibiting inhibitory potencies 4−105-fold higher toward hAChE than toward hBChE, albeit still maintaining potent hBChE inhibitory activity, with IC_{50} values in the nanomolar range (Table 1). No clear trends were found regarding the influence of the presence or absence of a chlorine atom at the tacrine unit or the length of the linker on the hBChE inhibitory activity. The presence of a methylamino group in the linker seemed to be beneficial for this activity, compounds (±)-**7c** and (±)-**8c** being 3- and 1.5-fold more potent than (±)-**7b** and (±)-**8b**, respectively, with an equivalent tether length. The (+)-(7*R*,11*R*)-enantiomer of heterodimer **8b** is more potent than the levorotatory enantiomer, but in the case of **7b**, both enantiomers turned out to be equipotent. The most potent huprine−tacrine heterodimers as hBChE inhibitors, i.e., (±)-**7a**, (±)-**7f**, and (±)-**8e**, are 6−7-fold more potent than (±)-huprine Y and equipotent with respect to tacrine.

Aβ Self-Aggregation Inhibition. The inhibitory activity of huprine−tacrine heterodimers on Aβ self-induced aggregation was also evaluated using a thioflavin T-based fluorometric assay.[42] Huprine−tacrine heterodimers significantly inhibit the self-induced Aβ aggregation when tested at a concentration 5-fold lower than that of Aβ, exhibiting percentages of inhibition ranging from 28 to 64%, clearly higher than those found for the parent huprine Y and tacrine (Table 1). The presence of an unsubstituted tacrine unit leads to a higher potency, heterodimers **7** being ∼1.5−2-fold more potent than their 6-chlorotacrine-based counterparts **8**. In the first series, the inhibitory activity toward Aβ self-aggregation peaks at a tether length of eight methylenes whereas the presence of a methylamino group in the linker is detrimental to this activity, and no difference in potency was found for enantiomers. In the 6-chlorotacrine-based series, the length of the linker and the presence of a methylamino group in the linker had a weaker influence on this activity, but a significant difference in potency was found for both enantiomers of compound **8b**, in favor of the dextrorotatory enantiomer.

It is worth noting that the most potent huprine−tacrine heterodimers toward Aβ self-induced aggregation, i.e., compounds (±)-**7b**, (−)-**7b**, (+)-**7b**, (±)-**7d**, and (±)-**7e**, have IC_{50} values below or close to 10 μM.

As a final remark, considering the overall inhibitory activity of huprine−tacrine heterodimers on AChE-induced and self-induced Aβ aggregation, the possibility that the inhibitory activity against self-induced Aβ aggregation does not partially contribute to the inhibitory action against the AChE-induced one cannot be unequivocally excluded.

BACE-1 Inhibition. BACE-1 is involved in the first and rate-limiting step of formation of Aβ from APP. Because Aβ aggregation is partially a concentration-dependent event, reduction of brain Aβ levels by inhibition of BACE-1 might be of utmost importance for a disease-modifying anti-Alzheimer therapeutic approach.[43] Indeed, brain Aβ production, amyloid pathology, and cognitive deficits are abrogated in BACE-1 knockout mice overexpressing APP.[44] Some concerns about potential mechanism-based toxicity,[45] which might be prevented by a partial inhibition of BACE-1, have arisen. Encouragingly, heterozygous BACE-1 knockout APP transgenic mice with an only 15% reduction in the level of brain Aβ showed a dramatic reduction in brain amyloid burden at old age.[44]

The ability of the huprine−tacrine heterodimers to inhibit in vitro human recombinant BACE-1 was determined at a single concentration (5 μM) using a fluorometric assay.[46] 6-Chlorotacrine-based heterodimers were found to exhibit an important BACE-1 inhibitory activity, with percentages of inhibition ranging from 18 to 47% at 5 μM (Table 1), clearly higher than that of huprine Y and tacrine. In this series, neither the length of the linker nor the configuration of the huprine moiety in the enantiopure heterodimers had an influence on BACE-1 inhibitory activity, most of these heterodimers displaying very similar percentages of inhibition between 40 and 47%, whereas only the presence of a methylamino group in the linker was clearly detrimental for BACE-1 inhibition. Conversely, with the sole exception of the longer homologues (±)-**7e** and (±)-**7f**, heterodimers bearing an unsubstituted tacrine unit were inactive toward BACE-1.

The IC_{50} for BACE-1 inhibition was determined for most of the active heterodimers, namely, (±)-**7f**, (−)-**8b**, (+)-**8b**, and (±)-**8d**−**f**, and found to lie within the range from 5 to 7 μM (Table 1). Thus, huprine−tacrine heterodimers exhibit a BACE-1 inhibitory activity very similar to that found for the prototypic dual-binding site AChEI bis(7)-tacrine (IC_{50} = 7.5 μM)[47] and can be considered moderately potent inhibitors of BACE-1. Moreover, on the basis of the structural similarity between huprine−tacrine heterodimers and bis(7)tacrine, which was found to reduce BACE-1 intracellular activity at a concentration of 1 μM,[47] we are confident that these heterodimers can be active in more complex biological systems, being able to cross the cell membrane and therefore exerting the same activity in cell cultures.

Brain Penetration. In Vitro Blood−Brain Barrier Permeation Assay. The development of drugs intented to act in the CNS has to contend with the need to efficiently cross the BBB. Brain penetration of the huprine−tacrine heterodimers was predicted using a parallel artificial membrane permeation assay, namely the widely known PAMPA−BBB assay.[48] The in vitro permeability (P_e) of racemic huprine−tacrine heterodimers through a lipid extract of porcine brain was determined by using a 70:30 phosphate-buffered saline (PBS)/EtOH mixture. The assay was validated by comparing the experimental permeability with the reported values of 15 commercial drugs that gave a good linear correlation: $P_e(\text{exp}) = 1.99P_e(\text{lit.}) + 1.07$ ($R^2 = 0.92$) (Tables S1 and S2 and Figure S8 of the Supporting Information). From this equation and taking into account the limits established by Di et al. for BBB permeation,[48] we established that compounds with permeability values of $>9.0 \times 10^{-6}$ cm/s should cross the BBB. All the huprine−tacrine heterodimers showed permeability values above this limit, with the sole exceptions of (±)-**7e** and (±)-**8c**, for which an uncertain BBB permeation has been predicted (Tables S1 and S2 of the Supporting Information). In general, heterodimers bearing a 6-chloro-substituted tacrine unit seem to be more brain permeable than their counterparts bearing an unsubstituted tacrine unit. Also, brain permeability increases with an increase in tether length, heterodimers (±)-**7f** and (±)-**8f** being the most permeable of each series. Not unexpectedly, introduction of a protonatable methylamino group into the linker leads to a decreased permeability relative to that of the corresponding heterodimer with an oligomethylene linker of equivalent length.

These results reveal that most huprine−tacrine heterodimers could cross the BBB and reach their multiple pharmacological targets located in the CNS, which has been confirmed for huprines in in vivo[36] and ex vivo[28] studies.

Ex Vivo Brain Penetration Study. To confirm the brain permeability of the huprine−tacrine heterodimers predicted by the PAMPA−BBB assay, compounds (±)-**7d** and (±)-**8d** were subjected to an ex vivo determination of their AChE inhibitory activity using the same methodology and conditions previously set up for huprines.[28] In this assay, huprine−tacrine heterodimers were administered intraperitoneally (ip) to OF1 mice at a single dose of 10 μmol/kg 20 min before the animals were sacrificed, and the percentage of brain AChE inhibition versus untreated controls was measured. Heterodimers (±)-**7d** and (±)-**8d** were found to inhibit mouse brain AChE activity by 30.0 ± 3.3 and 28.5 ± 3.7%, respectively, relative to control nontreated animals. The parent (±)-huprine Y had been reported to inhibit brain AChE activity under these conditions by 59.2 ± 8.2%. The lower potency of (±)-**7d** and (±)-**8d** relative to that of the parent huprine Y could be ascribed, in part, to their slightly lower potency found in vitro (Table 1), but also to the fact that in this assay we used the experimental conditions that were optimized for huprines. Irrespective of the fact that perhaps a greater activity could be observed for huprine−tacrine heterodimers (±)-**7d** and (±)-**8d** under optimized conditions, their significant inhibition of brain mouse AChE after their ip administration clearly demonstrates that they are able to cross the BBB in vivo.

CONCLUSION

We have developed a family of 16 heterodimeric compounds consisting of a unit of racemic or enantiopure huprine Y linked to a unit of tacrine or 6-chlorotacrine through an oligomethylene chain of 6−10 methylene groups or a 4-methyl-4-azaheptamethylene chain. These huprine−tacrine heterodimers have been designed to simultaneously interact with both the active and peripheral sites of AChE and in some cases also with aromatic residues at the midgorge of the enzyme. The dual-site binding of these compounds to hAChE results in a highly potent inhibition of the catalytic activity of hAChE and, more importantly, in an in vitro neutralization of the pathological chaperoning effect of this enzyme toward Aβ and PrP aggregation. To the best of our knowledge, this is the first report of a structural family exhibiting this dual anti-amyloidogenic action. Because Aβ aggregation and PrP aggregation are key early pathogenic events in AD and prion diseases, the dual action of huprine−tacrine heterodimers is of great interest for a potential disease-modifying treatment of these disorders. Additionally, huprine−tacrine heterodimers have been found to display other pharmacological effects resulting from their action on biological targets other than AChE, namely, a potent inhibitory activity on BChE and a significant inhibitory activity toward self-induced Aβ aggregation and BACE-1, which should reinforce their symptomatic and disease-modifying effects, respectively, in the context of AD treatment, even though it should be noted that more balanced activities at the different targets would be desirable. Huprine−tacrine heterodimers are able to cross the BBB, as predicted by the PAMPA−BBB assay and demonstrated for two selected compounds in ex vivo experiments, thereby having access to their different biological targets in the CNS, from which a plethora of pharmacological effects result. Taken together, the data show that huprine−tacrine heterodimers can be considered very promising lead compounds for AD and prion diseases.

EXPERIMENTAL SECTION

The analytical samples of all of the huprine−tacrine heterodimers that were subjected to pharmacological evaluation possess a purity of ≥95% as evidenced by their elemental analyses. Enantiopure huprine−tacrine heterodimers possess an enantiomeric excess of >99% as evidenced by chiral HPLC. The synthetic procedure for the preparation of the huprine−tacrine heterodimers is exemplified through the synthesis of (−)-**7b**.

(−)-(7*S*,11*S*)-3-Chloro-6,7,10,11-tetrahydro-9-methyl-12-({7-[(1,2,3,4-tetrahydroacridin-9-yl)amino]heptyl}amino)-7,11-methanocycloocta[*b*]quinoline Dihydrochloride [(−)-7b·2HCl] from (−)-Huprine Y. A mixture of finely powdered KOH (85% pure reagent, 225 mg, 3.42 mmol, 1.6 equiv), (−)-huprine Y [(−)-**6**][34] (323 mg, 1.14 mmol, 1 equiv), and 4 Å molecular sieves (approximately 690 mg) in dry DMSO (4 mL) was thoroughly stirred for 1 h and heated with a heatgun every 10 min and for an additional 1 h at room temperature. The resulting mixture was added dropwise over 2 h to a

dx.doi.org/10.1021/jm200840c | J. Med. Chem. 2012, 55, 661−669

mixture of haloalkyltacrine **4b** (515 mg, 1.37 mmol, 1.2 equiv) in dry DMSO (5 mL). The reaction mixture was vigorously stirred at room temperature for 3 days, diluted with water (200 mL), treated with NaOH pellets until an alkaline pH was reached, and extracted with AcOEt (3 × 160 mL). The combined organic extracts were washed with water (3 × 150 mL), dried with anhydrous Na_2SO_4, and evaporated at reduced pressure to give a brown oily residue (549 mg), which was subjected to column chromatography (35−70 mesh silica gel, 100:0.2 CH_2Cl_2/50% aqueous NH_4OH mixture). Starting (−)-**6** (63 mg), β-elimination byproduct (25 mg), a mixture of β-elimination byproduct and heterodimer (−)-**7b** in a ratio of 1:99 (285 mg), and pure heterodimer (−)-**7b** (85 mg, 13% isolated yield, 56% total yield) were consecutively separated as yellowish oils.

A solution of (−)-**7b** (85 mg, 0.15 mmol) in CH_2Cl_2 (10 mL) was filtered through a polytetrafluoroethylene 0.45 μm filter and treated with an excess of a methanolic solution of HCl (0.65 N, 2.0 mL, 1.3 mmol), and the resulting solution was concentrated in vacuo to dryness. The solid was taken in MeOH (0.6 mL) and precipitated upon addition of AcOEt (1.6 mL). The precipitated solid was separated and dried at 65 °C and 15 Torr for 4 days to give (−)-**7b**·2HCl·2.75H_2O (75 mg) as a light brown solid: $[\alpha]^{20}_D = -139$ (c = 0.30, MeOH); >99% ee by chiral HPLC on the liberated base [CHIRALCEL OD-H column, 90:10:0.1 hexane/EtOH/Et_2NH mixture, flow rate of 0.2 mL/min, λ = 254 nm; (−)-**7b**, t_R = 55.27 min, k'_1 = 2.54; (+)-**7b**, t_R = 61.77 min, k'_2 = 2.96; α = 1.16, res. = 6.7]; mp 237−239 °C (3:8 MeOH/AcOEt); IR (KBr) ν 3600−2500 (maxima at 3405, 3234, 3049, 2927, 2855, and 2773 cm^{-1}; N^+-H, N-H, and C-H st), 1628, 1617, 1583, 1572, 1534 (ar-C-C and ar-C-N st) cm^{-1}. The ^1H and ^{13}C NMR spectra were identical to those described for (±)-**7b**·2HCl.[24] HRMS calcd for $C_{37}H_{43}{}^{35}ClN_4$ + H: 579.3249. Found: 579.3240. Anal. ($C_{37}H_{43}ClN_4$·2HCl·2.75H_2O) C, H, N, Cl.

■ ASSOCIATED CONTENT

Supporting Information

Experimental procedures (chemistry and biochemical, brain penetration, and molecular modeling studies), fluorescence micrographs of the effect of huprine−tacrine heterodimers on AChE-induced coumarin−PrP106−126 aggregation, and figures displaying additional data from kinetic, molecular dynamics, and PAMPA−BBB studies. This material is available free of charge via the Internet at http://pubs.acs.org.

■ AUTHOR INFORMATION

Corresponding Author

*Phone: +34+934024533. Fax: +34+934035941. E-mail: dmunoztorrero@ub.edu.

■ ACKNOWLEDGMENTS

Financial support from the Ministerio de Ciencia e Innovación (MICINN) and FEDER (CTQ2008-03768/PPQ, SAF2009-10553, SAF2008-05595, and SAF2006-01249), Generalitat de Catalunya (GC) (2005SGR00180, 2009SGR1396, 2009SGR0843, and 2009SGR249), EU's 7FP funding (BISNES, NMP-2007-1.1-1, GA no. 214538), and fellowships for C.G. (IBUB) and E.V. (GC) are acknowledged. We thank Isabel Delgado for technical support.

■ ABBREVIATIONS

Aβ, β-amyloid peptide; AChE, acetylcholinesterase; AChEI, acetylcholinesterase inhibitor; AD, Alzheimer's disease; apoE, apolipoprotein E; APP, amyloid precursor protein; BACE-1, β-secretase; BBB, blood−brain barrier; BChE, butyrylcholinesterase; CNS, central nervous system; hAChE, human acetylcholinesterase; hBChE, human butyrylcholinesterase; MD, molecular dynamics; PAMPA, parallel artificial membrane permeation assay; PBS, phosphate-buffered saline; PDB, Protein Data Bank; PrP^C, cellular prion protein; PrP^{Sc}, scrapie prion protein; SIE, solvent interaction energy; *Tc*AChE, *T. californica* acetylcholinesterase

■ REFERENCES

(1) Wimo, A.; Prince, M. *World Alzheimer Report 2010. The global economic impact of dementia*; Alzheimer's Disease International (http://www.alz.co.uk).

(2) Cobb, N. J.; Surewicz, W. K. Prion diseases and their biochemical mechanisms. *Biochemistry* **2009**, *48*, 2574−2585.

(3) Wisniewski, T.; Sigurdsson, E. M. Therapeutic approaches for prion and Alzheimer's disease. *FEBS J.* **2007**, *274*, 3784−3798.

(4) Barnham, K. J.; Cappai, R.; Beyreuther, K.; Masters, C. L.; Hill, A. F. Delineating common molecular mechanisms in Alzheimer's and prion diseases. *Trends Biochem. Sci.* **2006**, *31*, 465−472.

(5) Soto, C. Protein misfolding and disease; protein refolding and therapy. *FEBS Lett.* **2001**, *498*, 204−207.

(6) Soto, C.; Kascsak, R. J.; Saborío, G. P.; Aucouturier, P.; Wisniewski, T.; Prelli, F.; Kascsak, R.; Mendez, E.; Harris, D. A.; Ironside, J.; Tagliavini, F.; Carp, R. I.; Frangione, B. Reversion of prion protein conformational changes by synthetic β-sheet breaker peptides. *Lancet* **2000**, *355*, 192−197.

(7) Zhang, H.-Y. Same causes, same cures. *Biochem. Biophys. Res. Commun.* **2006**, *351*, 578−581.

(8) Bartolini, M.; Andrisano, V. Strategies for the inhibition of protein aggregation in human diseases. *ChemBioChem* **2010**, *11*, 1018−1035.

(9) Re, F.; Airoldi, C.; Zona, C.; Masserini, M.; La Ferla, B.; Quattrocchi, N.; Nicotra, F. β amyloid aggregation inhibitors: Small molecules as candidate drugs for therapy of Alzheimer's disease. *Curr. Med. Chem.* **2010**, *17*, 2990−3006.

(10) Tran, H. N. A.; Bongarzone, S.; Carloni, P.; Legname, G.; Bolognesi, M. L. Synthesis and evaluation of a library of 2,5-bisdiamino-benzoquinone derivatives as probes to modulate protein-protein interactions in prions. *Bioorg. Med. Chem. Lett.* **2010**, *20*, 1866−1868.

(11) Ma, J.; Yee, A.; Brewer, H. B. Jr.; Das, S.; Potter, H. Amyloid-associated proteins α1-antichymotrypsin and apolipoprotein E promote assembly of Alzheimer β-protein into filaments. *Nature* **1994**, *372*, 92−94.

(12) Boyett, K. W.; DiCarlo, G.; Jantzen, P. T.; Jackson, J.; O'Leary, C.; Wilcock, D.; Morgan, D.; Gordon, M. N. Increased fibrillar β-amyloid in response to human C1q injections into hippocampus and cortex of APP + PS1 transgenic mice. *Neurochem. Res.* **2003**, *28*, 83−93.

(13) Inestrosa, N. C.; Alvarez, A.; Pérez, C. A.; Moreno, R. D.; Vicente, M.; Linker, C.; Casanueva, O. I.; Soto, C.; Garrido, J. Acetylcholinesterase accelerates assembly of amyloid-β-peptides into Alzheimer's fibrils: Possible role of the peripheral site of the enzyme. *Neuron* **1996**, *16*, 881−891.

(14) Bales, K. R.; Verina, T.; Cummins, D. J.; Du, Y.; Dodel, R. C.; Saura, J.; Fishman, C. E.; DeLong, C. A.; Piccardo, P.; Petegnief, V.; Ghetti, B.; Paul, S. M. Apolipoprotein E is essential for amyloid deposition in the APPV717F transgenic mouse model of Alzheimer's disease. *Proc. Natl. Acad. Sci. U.S.A.* **1999**, *96*, 15233−15238.

(15) Rees, T. M.; Berson, A.; Sklan, E. H.; Younkin, L.; Younkin, S.; Brimijoin, S.; Soreq, H. Memory deficits correlating with acetylcholinesterase splice shift and amyloid burden in doubly transgenic mice. *Curr. Alzheimer Res.* **2005**, *2*, 291−300.

(16) De Ferrari, G. V.; Canales, M. A.; Shin, I.; Weiner, L. M.; Silman, I.; Inestrosa, N. C. A structural motif of acetylcholinesterase that promotes amyloid β-peptide fibril formation. *Biochemistry* **2001**, *40*, 10447−10457.

(17) Naslund, J.; Thyberg, J.; Tjernberg, L. O.; Wernstedt, C.; Karlstrom, A. R.; Bogdanovic, N.; Gandy, S. E.; Lannfelt, L.; Terenius, L.; Nordstedt, C. Characterization of stable complexes involving

apolipoprotein E and the amyloid β peptide in Alzheimer's disease brain. *Neuron* **1995**, *15*, 219−228.
(18) Cavalli, A.; Bolognesi, M. L.; Capsoni, S.; Andrisano, V.; Bartolini, M.; Margotti, E.; Cattaneo, A.; Recanatini, M.; Melchiorre, C. A small molecule targeting the multifactorial nature of Alzheimer's disease. *Angew. Chem., Int. Ed.* **2007**, *46*, 3689−3692.
(19) García-Palomero, E.; Muñoz, P.; Usan, P.; Garcia, P.; De Austria, C.; Valenzuela, R.; Rubio, L.; Medina, M.; Martínez, A. Potent β-amyloid modulators. *Neurodegener. Dis.* **2008**, *5*, 153−156.
(20) Spuch, C.; Antequera, D.; Fernandez-Bachiller, M. I.; Rodríguez-Franco, M. I.; Carro, E. A new tacrine-melatonin hybrid reduces amyloid burden and behavioral deficits in a mouse model of Alzheimer's disease. *Neurotoxic. Res.* **2010**, *17*, 421−431.
(21) Pera, M.; Román, S.; Ratia, M.; Camps, P.; Muñoz-Torrero, D.; Colombo, L.; Manzoni, C.; Salmona, M.; Badia, A.; Clos, M. V. Acetylcholinesterase triggers the aggregation of PrP 106−126. *Biochem. Biophys. Res. Commun.* **2006**, *346*, 89−94.
(22) Pera, M.; Martínez-Otero, A.; Colombo, L.; Salmona, M.; Ruiz-Molina, D.; Badia, A.; Clos, M. V. Acetylcholinesterase as an amyloid enhancing factor in PrP82−146 aggregation process. *Mol. Cell. Neurosci.* **2009**, *40*, 217−224.
(23) Bartolini, M.; Bertucci, C.; Cavrini, V.; Andrisano, V. β-Amyloid aggregation induced by human acetylcholinesterase: Inhibition studies. *Biochem. Pharmacol.* **2003**, *65*, 407−416.
(24) Camps, P.; Formosa, X.; Muñoz-Torrero, D.; Petrignet, J.; Badia, A.; Clos, M. V. Synthesis and pharmacological evaluation of huprine-tacrine heterodimers: Subnanomolar dual binding site acetylcholinesterase inhibitors. *J. Med. Chem.* **2005**, *48*, 1701−1704.
(25) Camps, P.; Cusack, B.; Mallender, W. D.; El Achab, R.; Morral, J.; Muñoz-Torrero, D.; Rosenberry, T. L. Huprine X is a novel high-affinity inhibitor of acetylcholinesterase that is of interest for the treatment of Alzheimer's disease. *Mol. Pharmacol.* **2000**, *57*, 409−417.
(26) Pang, Y.-P.; Quiram, P.; Jelacic, T.; Hong, F.; Brimijoin, S. Highly potent, selective, and low cost bis-tetrahydroaminacrine inhibitors of acetylcholinesterase. *J. Biol. Chem.* **1996**, *271*, 23646−23649.
(27) Savini, L.; Gaeta, A.; Fattorusso, C.; Catalanotti, B.; Campiani, G.; Chiasserini, L.; Pellerano, C.; Novellino, E.; McKissic, D.; Saxena, A. Specific targeting of acetylcholinesterase and butyrylcholinesterase recognition sites. Rational design of novel, selective, and highly potent cholinesterase inhibitors. *J. Med. Chem.* **2003**, *46*, 1−4.
(28) Camps, P.; El Achab, R.; Morral, J.; Muñoz-Torrero, D.; Badia, A.; Baños, J. E.; Vivas, N. M.; Barril, X.; Orozco, M.; Luque, F. J. New tacrine-huperzine A hybrids (huprines): Highly potent tight-binding acetylcholinesterase inhibitors of interest for the treatment of Alzheimer's disease. *J. Med. Chem.* **2000**, *43*, 4657−4666.
(29) Dvir, H.; Wong, D. M.; Harel, M.; Barril, X.; Orozco, M.; Luque, F. J.; Muñoz-Torrero, D.; Camps, P.; Rosenberry, T. L.; Silman, I.; Sussman, J. L. 3D Structure of *Torpedo californica* acetylcholinesterase complexed with huprine X at 2.1 Å resolution: Kinetic and molecular dynamics correlates. *Biochemistry* **2002**, *41*, 2970−2981.
(30) Carlier, P. R.; Chow, E. S.-H.; Han, Y.; Liu, J.; El Yazal, J.; Pang, Y.-P. Heterodimeric tacrine-based acetylcholinesterase inhibitors: Investigating ligand-peripheral site interactions. *J. Med. Chem.* **1999**, *42*, 4225−4231.
(31) Ma, M.; Mehta, J.; Williams, L. D.; Carlier, P. R. Pd-catalyzed amination as an alternative to nucleophilic aromatic substitution for the synthesis of *N*-alkyltacrines and analogs. *Tetrahedron Lett.* **2011**, *52*, 916−919.
(32) Ronco, C.; Jean, L.; Outaabout, H.; Renard, P.-Y. Palladium-catalyzed preparation of *N*-alkylated tacrine and huprine compounds. *Eur. J. Org. Chem.* **2011**, 302−310.
(33) Gregor, V. E.; Emmerling, M. R.; Lee, C.; Moore, C. J. The synthesis and *in vitro* acetylcholinesterase and butyrylcholinesterase inhibitory activity of tacrine (Cognex®) derivatives. *Bioorg. Med. Chem. Lett.* **1992**, *2*, 861−864.
(34) Camps, P.; Contreras, J.; Font-Bardia, M.; Morral, J.; Muñoz-Torrero, D.; Solans, X. Enantioselective synthesis of tacrine-huperzine A hybrids. Preparative chiral MPLC separation of their racemic mixtures and absolute configuration assignments by X-ray diffraction analysis. *Tetrahedron: Asymmetry* **1998**, *9*, 835−849.
(35) Ellman, G. L.; Courtney, K. D.; Andres, V. Jr.; Featherstone, R. M. A new and rapid colorimetric determination of acetylcholinesterase activity. *Biochem. Pharmacol.* **1961**, *7*, 88−95.
(36) Hedberg, M. M.; Clos, M. V.; Ratia, M.; Gonzalez, D.; Unger Lithner, C.; Camps, P.; Muñoz-Torrero, D.; Badia, A.; Giménez-Llort, L.; Nordberg, A. Effect of huprine X on β-amyloid, synaptophysin and α7 neuronal nicotinic acetylcholine receptors in the brain of 3xTg-AD and APPswe transgenic mice. *Neurodegener. Dis.* **2010**, *7*, 379−388.
(37) Rydberg, E. H.; Brumshtein, B.; Greenblatt, H. M.; Wong, D. M.; Shaya, D.; Williams, L. D.; Carlier, P. R.; Pang, Y.-P.; Silman, I.; Sussman, J. L. Complexes of alkylene-linked tacrine dimers with *Torpedo californica* acetylcholinesterase: Binding of bis(5)-tacrine produces a dramatic rearrangement in the active site gorge. *J. Med. Chem.* **2006**, *49*, 5491−5500.
(38) Harel, M.; Schalk, I.; Ehret-Sabatier, L.; Bouet, F.; Goeldner, M.; Hirth, C.; Axelsen, P. H.; Silman, I.; Sussman, J. L. Quaternary ligand binding to aromatic residues in the active-site gorge of acetylcholinesterase. *Proc. Natl. Acad. Sci. U.S.A.* **1993**, *90*, 9031−9035.
(39) Cui, Q.; Sulea, T.; Schrag, J. D.; Munger, C.; Hung, M.-N.; Nam, M.; Cygler, M.; Purisima, E. O. Molecular dynamics-solvated interaction energy studies of protein-protein interactions: The MP1-p14 scaffolding complex. *J. Mol. Biol.* **2008**, *379*, 787−802.
(40) Lane, R. M.; Potkin, S. G.; Enz, A. Targeting acetylcholinesterase and butyrylcholinesterase in dementia. *Int. J. Neuropsychopharmacol.* **2006**, *9*, 101−124.
(41) Elsinghorst, P. W.; Cieslik, J. S.; Mohr, K.; Tränkle, C.; Gütschow, M. First gallamine-tacrine hybrid: Design and characterization at cholinesterases and the M_2 muscarinic receptor. *J. Med. Chem.* **2007**, *50*, 5685−5695.
(42) Bartolini, M.; Bertucci, C.; Bolognesi, M. L.; Cavalli, A.; Melchiorre, C.; Andrisano, V. Insight into the kinetic of amyloid β(1−42) peptide self-aggregation: Elucidation of inhibitors' mechanism of action. *ChemBioChem* **2007**, *8*, 2152−2161.
(43) De Strooper, B.; Vassar, R.; Golde, T. The secretases: Enzymes with therapeutic potential in Alzheimer's disease. *Nat. Rev. Neurol.* **2010**, *6*, 99−107.
(44) McConlogue, L.; Buttini, M.; Anderson, J. P.; Brigham, E. F.; Chen, K. S.; Freedman, S. B.; Games, D.; Johnson-Wood, K.; Lee, M.; Zeller, M.; Liu, W.; Motter, R.; Sinha, S. Partial reduction of BACE1 has dramatic effects on Alzheimer plaque and synaptic pathology in APP transgenic mice. *J. Biol. Chem.* **2007**, *282*, 26326−26334.
(45) Hu, X.; Hicks, C. W.; He, W.; Wong, P.; Macklin, W. B.; Trapp, B. D.; Yan, R. BACE1 modulates myelination in the central and peripheral nervous system. *Nat. Neurosci.* **2006**, *9*, 1520−1525.
(46) Hanessian, S.; Yun, H.; Hou, Y.; Yang, G.; Bayrakdarian, M.; Therrien, E.; Moitessier, N.; Roggo, S.; Veenstra, S.; Tintelnot-Blomley, M.; Rondeau, J.-M.; Ostermeier, C.; Strauss, A.; Ramage, P.; Paganetti, P.; Neumann, U.; Betschart, C. Structure-based design, synthesis, and memapsin 2 (BACE) inhibitory activity of carbocyclic and heterocyclic peptidomimetics. *J. Med. Chem.* **2005**, *48*, 5175−5190.
(47) Fu, H.; Li, W.; Luo, J.; Lee, N. T. K.; Li, M.; Tsim, K. W. K.; Pang, Y.; Youdim, M. B. H.; Han, Y. Promising anti-Alzheimer's dimer bis(7)-tacrine reduces β-amyloid generation by directly inhibiting BACE-1 activity. *Biochem. Biophys. Res. Commun.* **2008**, *366*, 631−636.
(48) Di, L.; Kerns, E. H.; Fan, K.; McConnell, O. J.; Carter, G. T. High throughput artificial membrane permeability assay for blood-brain barrier. *Eur. J. Med. Chem.* **2003**, *38*, 223−232.